COMPUTATIONAL MECHANICS 2021
36th conference with international participation
Srní
November 8 - 10, 2021

Aerodynamic wind tunnel testing of U-beams

S. Hračov[a], M. Macháček[a]

[a] *Institute of Theoretical and Applied Mechanics, Czech Academy of Sciences, Prosecká 76, 19000 Prague, Czech Republic*

The proposed paper presents the outcomes from the experimental aerodynamic testing of the slender beams with U-shaped cross section, which is typical e.g., for conveys, the bridge decks with the wind barriers or the footbridges with the railings. In particular, two sets of six U - beams having identical ratio of the along-wind to the across-wind dimension *B/D* = 2:1, but different porosity and depth of their U-shaped cross sections were analysed in order to determine their potential galloping susceptibility. The tests were carried out in the smooth flow conditions in the closed-circuit climatic wind tunnel of ITAM AS CR in Telč in the Czech Republic. The assessment of the proneness was performed based on the quasi-steady theory [3], i.e. on the analysis of a sign of a slope of the experimentally obtained transverse force coefficient, C_{Fy}, around the zero angle of the wind attack, α.

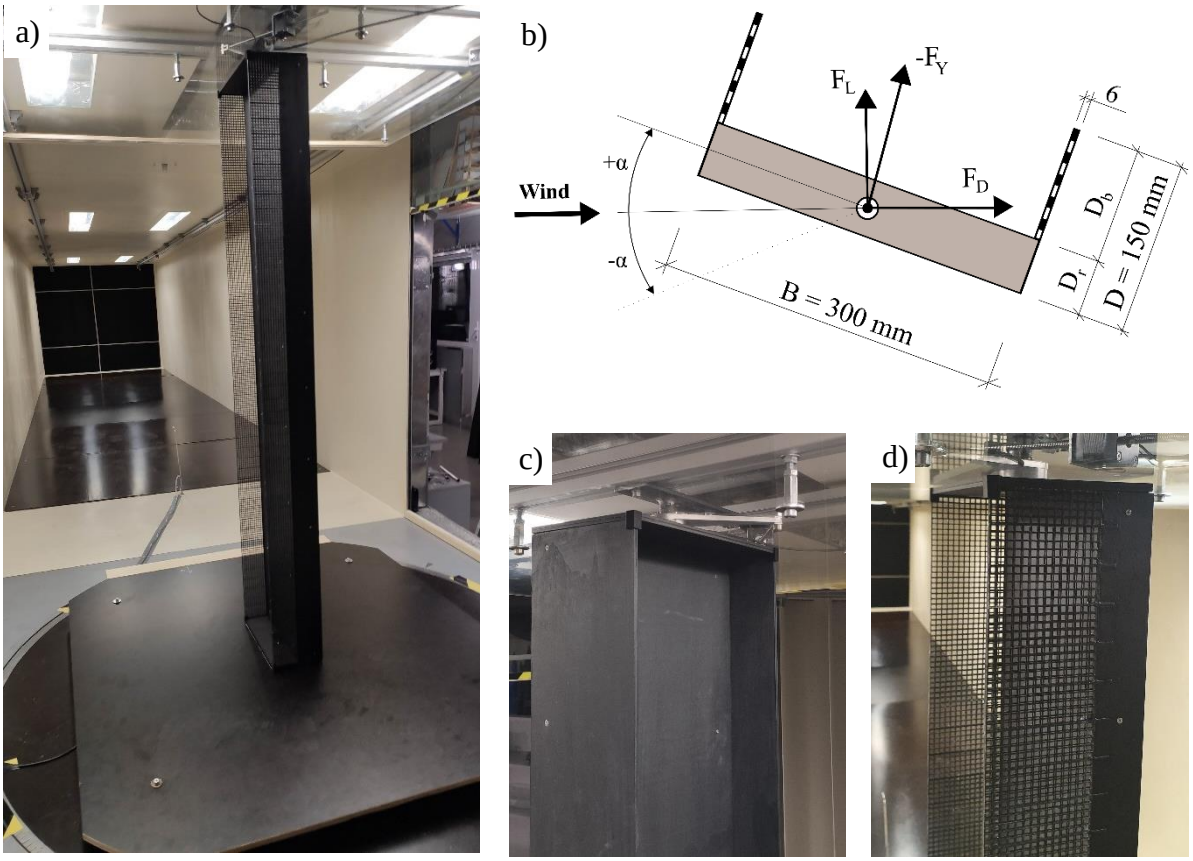

Fig. 1. (a) Photo of the porous U-shaped beam in the wind tunnel (B/D_r = 4:1, p= 75%), (b) Schema of the U-profile, (c) Snapshot of the non-porous U-profile (B/D_r = 4:1), (d) Snapshot of the U-profile (B/D_r = 6:1) with porosity p = 75%

All 160 cm long experimental specimens (beams) were assembled from a wooden rectangular prism and a pair of the plastic flanges. The basic geometry and dimensions of their U-shaped cross section are schematically depicted in Fig. 1b. The first set of six U-beams was constructed from the rectangular prism with B/D_r = 4:1, thus had the depth, D_b, equal to one-fourth of the width, B. For the second set of U-beams, which was characterized by D_b equal to one third of B, the rectangular prism with B/D_r = 6:1 was used. The individual U-beams in each set differed only in the level of the flange porosity. In total five levels of porosity ranging from 0 % to almost 100 % were analysed. The flanges were built from two plastic nets with certain degree of porosity that were glued onto the frontal and rear sides of a tiny plastic frame. All nets had an axial 7 mm square grid. For comparison purposes, also the rectangular prisms with side ratios B/D = 2:1, 4:1 and 6:1 and specimens with the attached frame only, i.e., without the nets, were tested.

All models were placed vertically into the measuring part of the aerodynamic test section of the wind tunnel, which is 1.9 m wide and 1.8 m high. The models were enclosed between wooden and plastic end-plates to enforce bidimensional flow conditions, see Fig. 1a. Two load cells ATI Industrial Automation sensors Mini 40 were used for measuring the aerodynamic drag and lift forces F_L and F_D caused on the bodies of the specimens by the wind load for the angles of wind attack, α, in the range from -15° to +15°. These sensors were fixed to the upper and lower ends of the specimens and to the specially designed synchronized rotation mechanisms, that enabled rotation of the specimens with the very small angular step, $\Delta\alpha = 0.2°$. Thus, the alternation of aerodynamic forces with the changing angle, α, can be detected very precisely. The data from the sensors were recorded for 60 seconds, which revealed as sufficient with respect of the ergodicity and stationarity of the process, with a sampling frequency f_s = 1000 Hz. All wind tunnel tests were conducted in a nominal smooth flow with minimal turbulence intensity around 1%. The independence of the aerodynamic force coefficients on the Reynolds number, Re, was successfully verified for wind velocity ranging from 4 ms^{-1} to 19 ms^{-1}. The tests were finally performed at a wind speed of about 14 m/s, i.e., corresponding to $Re = 2.8e^5$ normalized using along-wind dimension, B. Due to a higher blockage of the wind tunnel in the range of 7.9 % to 11.7 % depending on simulated angle of the wind attack, the corrections of the measured wind speeds, which was based on a comparison of the results of CFD simulations and measurements, were incorporated.

At first, the drag and lift coefficients, C_D and C_L, were evaluated from the mean values of the measured drag and lift forces, F_D and F_L, for all angles of wind attack according their definition, see e.g. [2]. The values of transverse force coefficient, C_{Fy}, were subsequently calculated from C_D and C_L based on the geometrical relations, see Fig. 1b or [2]. In Fig. 2 the obtained transverse force coefficient, C_{Fy}, is reported against the angle of attack for all analysed profiles. The upper graph of this figure is related to the set of beams with higher D_b, while the lower graph to the set of beams with lower D_b. All results are in these graphs normalized to the same height D = 150 mm.

The positive slope of C_{Fy} around zero angle of attack represents a necessary condition for galloping proneness of analysed profile [3]. The value of this slope corresponds also to the galloping stability parameter a_g [1], which is used for calculation of the onset galloping velocity. In engineering practise, the values of C_{Fy} are usually not explicitly determined as in this study and the coefficient a_g is calculated from the values of C_D and C_L according to formula

$$a_g = \frac{dC_{FY}}{d\alpha}\Big|_{(\alpha=0°)} = -\left(\frac{dC_L}{d\alpha} + C_D\right)\Big|_{(\alpha=0°)}. \quad (1)$$

This approach for evaluation of a_g was also adopted here. The value of the slope of C_L around zero angle was obtained by linear approximation of the values in the angular interval ranging from -1° to +1°. The only exception represented the beam with B/D_r = 6:1 and flange porosity

p = 75%, where only angular range from -0.5° to +0.5° was used. It must be noted, that a negative slope of the lift coefficient, C_L, around zero angle of the wind attack represents a necessary condition for possibility of the galloping proneness. The negative slope of C_L was determined for the rectangular prism with SR = 2, for all U-beams with flange porosity up to and including 75% and also for U-beam given by B/D_r = 4:1 and p = 90%. The values of the slope of C_L and C_D corresponding to the zero angle of wind attack are presented for all tested bodies in Table 1. Moreover, in this table also the galloping stability parameter, a_g, and the intervals of angles of attack around zero angle, $\Delta\alpha_{IP}$, for which C_{FY} has the positive slope, are given. Generally, the wider this interval is, the higher response of the body can be expected.

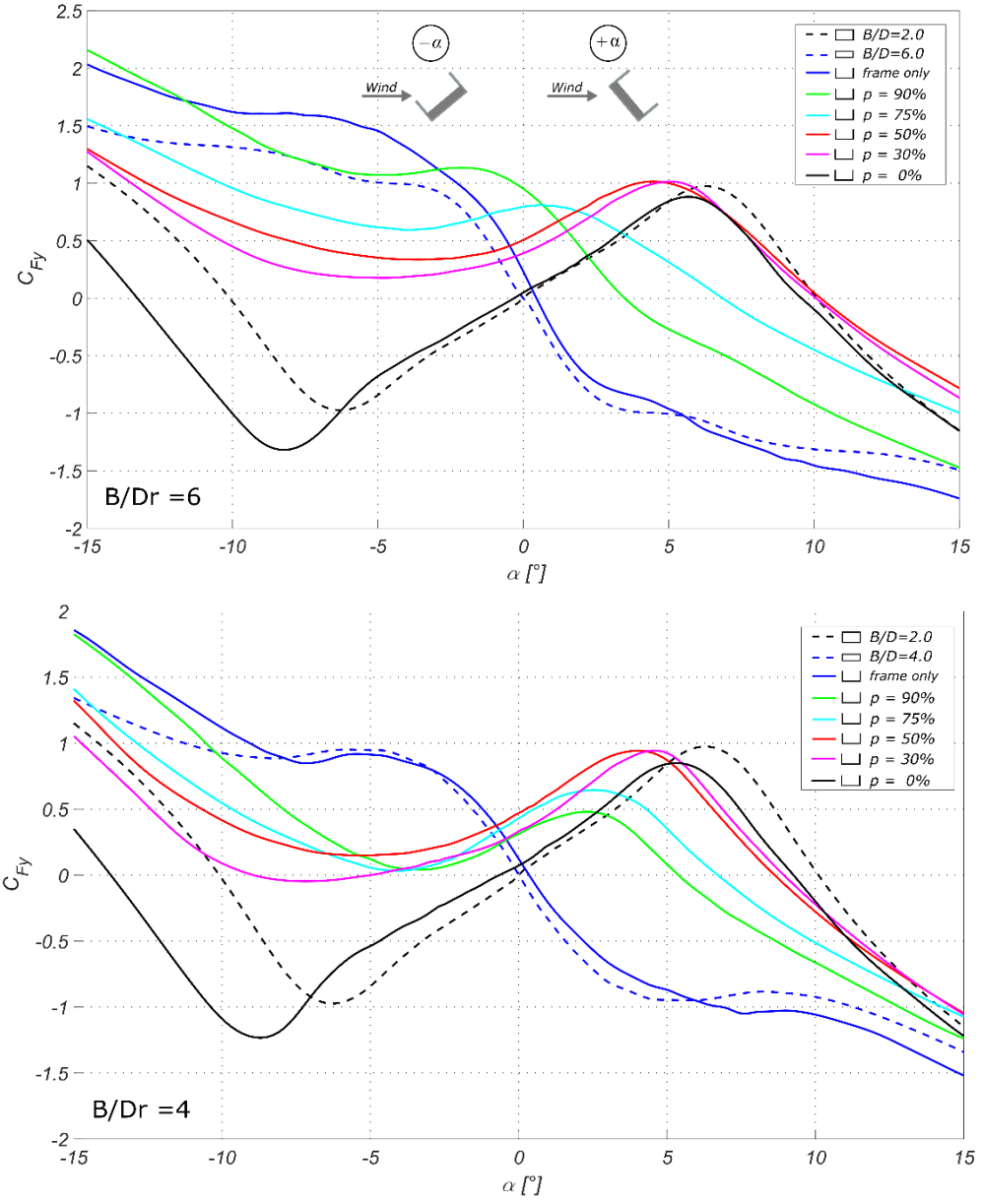

Fig. 2. The transverse force coefficient of the cylinders with rectangular and U-shaped cross-sections for various angles of wind attack

The analysis of the results showed the strong susceptibility of the rectangular prism with SR = 2 to the transversal galloping. The stability parameter, a_g, equal to very high value 9.81 was for this beam determined. Only slightly lower values of a_g were determined for U-beams with porosity up to and including 50 % regardless the depth, D_b, of their profiles. The onset galloping velocities for these U-profiles are expected to be very close.

Table 1. The aerodynamic parameters of tested profiles

Cross section	B/D [/]	B/Dr [/]	Porosity [%]	C_D (α=0°) [/]	$dC_L/d\alpha$ (α=0°) [/]	a_g [/]	$\Delta\alpha_{IP}$ [°]	$\langle\alpha_{IP-}; \alpha_{IP+}\rangle$ [°]
⊔	2	4	0	1.46	-8.94	7.48	14.0	⟨- 8.7; 5.3⟩
⊔	2	6	0	1.45	-9.60	8.15	13.8	⟨- 8.2; 5.6⟩
⊔	2	4	30	1.47	-8.26	6.79	11.6	⟨-7.1; 4.5⟩
⊔	2	6	30	1.49	-7.35	5.86	9.8	⟨-4.8; 5.0⟩
⊔	2	4	50	1.33	-8.66	7.33	9.4	⟨-5.3; 4.1⟩
⊔	2	6	50	1.42	-8.15	6.73	8.0	⟨-3.6; 4.4⟩
⊔	2	4	75	1.04	-8.60	7.56	6.6	⟨-4.1; 2.5⟩
⊔	2	6	75	1.04	-3.35	2.31	4.6	⟨-4.0; 0.6⟩
⊔	2	4	90	1.04	-7.53	6.48	5.6	⟨-3.4; 2.2⟩
⊔	2	6	90	0.94	9.42	-	-	-
⊔	2	4	frame	0.72	18.55	-	-	-
⊔	2	6	frame	0.52	26.92	-	-	-
□	2	2	0	1.48	-11.29	9.81	12.4	⟨-6.2; 6.2⟩
□	4	4	0	0.55	19.61	-	-	-
□	6	6	0	0.33	22.36	-	-	-

A more significant influence of D_b on a_g was identified only for U-beams with flange porosity higher than 50 %. While for lower D_b, i.e. B/D_r = 4:1, the coefficient a_g did not change substantially for all tested porosities, for lower D_b a significant reduction in a_g was observed for p = 75%. Finally, in the case of even higher porosity p = 90 % and lower D_b the profile can be considered as stable due to positive value of the slope of C_L. The positive slope of C_L and thus the resistance to galloping were also determined for rectangular prisms with SR = 4 and 6. The effect of the plastic frame onto the change of proneness to galloping of these rectangular cylinders was identified as minimal. The performed tests indicated that the interval, $\Delta\alpha_{IP}$, is decreasing with the increase in the flange porosity of U-profiles and with the increase in D_b. In the cases of non-porous U- profiles, this angular interval is even slightly wider than for rectangular prism with SR = 2.

The analysis of the results determined the beams with U-shaped cross sections with the side ratio SR = 2, depth D_b = *1/4 B* and flange porosity up to and including 90 % as potentially unstable from the point of view of transversal galloping. The proneness in terms of the expected value of critical wind velocity is almost in all cases comparable with the rectangular prism with SR = 2. In the case of U-beams with D_b = *1/3 B*, the susceptibility to galloping was determined for U-beams with porosity up to and including 75 %. However, for porosity equal to 75% a significant reduction of stability parameter affecting the value of onset galloping velocity was identified. The geometrically identical U-beams with porosities higher than 75% as well as the rectangular prisms with SR = 4 and 6 can be assumed as stable in terms of transverse galloping.

Acknowledgements

The kind support of Czech Scientific Foundation project No. 19-21817S and RVO 68378297 institutional support are gratefully acknowledged.

References

[1] Eurocode 1 – Actions on structures – Part 1-4: General actions –Wind actions.
[2] Hracov, S., Machacek, M., Susceptibility of U-profiles with different geometry and porosity to galloping, EASD Procedia EURODYN, 2020, pp. 621-630.
[3] Paidoussis, M.P., Price, S.J., de Langre, E., Fluid-structure interactions: cross-flow induced instabilities, Cambridge University Press, 2014.